pubs.acs.org/Biomac

Article

Gelatin-Based Hybrid Hydrogels as Matrices for Organoid Culture

Nathan Carpentier,[⊥] Shicheng Ye,[⊥] Maarten D. Delemarre, Louis Van der Meeren, André G. Skirtach, Luc J. W. van der Laan, Kerstin Schneeberger,* Bart Spee, Peter Dubruel, and Sandra Van Vlierberghe*

Cite This: *Biomacromolecules* 2024, 25, 590−604

Read Online

ACCESS | Metrics & More | Article Recommendations | Supporting Information

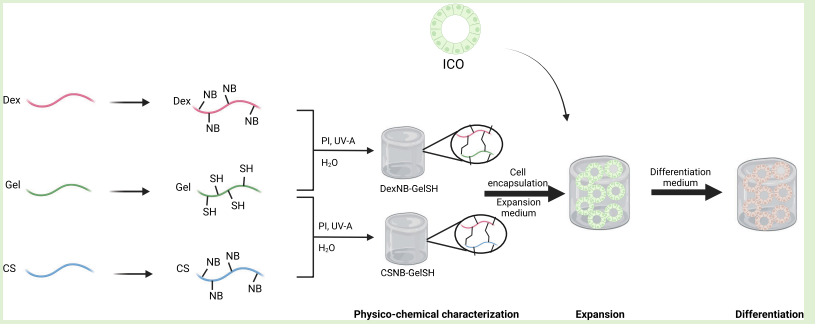

ABSTRACT: The application of liver organoids is very promising in the field of liver tissue engineering; however, it is still facing some limitations. One of the current major limitations is the matrix in which they are cultured. The mainly undefined and murine-originated tumor matrices derived from Engelbreth−Holm−Swarm (EHS) sarcoma, such as Matrigel, are still the standard culturing matrices for expansion and differentiation of organoids toward hepatocyte-like cells, which will obstruct its future clinical application potential. In this study, we exploited the use of newly developed highly defined hydrogels as potential matrices for the culture of liver organoids and compared them to Matrigel and two hydrogels that were already researched in the field of organoid research [i.e., polyisocyanopeptides, enriched with laminin−entactin complex (PIC-LEC) and gelatin methacryloyl (GelMA)]. The newly developed hydrogels are materials that have a physicochemical resemblance with native liver tissue. Norbornene-modified dextran cross-linked with thiolated gelatin (DexNB-GelSH) has a swelling ratio and macro- and microscale properties that highly mimic liver tissue. Norbornene-modified chondroitin sulfate cross-linked with thiolated gelatin (CSNB-GelSH) contains chondroitin sulfate, which is a glycosaminoglycan (GAG) that is present in the liver ECM. Furthermore, CSNB-GelSH hydrogels with different mechanical properties were evaluated. Bipotent intrahepatic cholangiocyte organoids (ICOs) were applied in this work and encapsulated in these materials. This research revealed that the newly developed materials outperformed Matrigel, PIC-LEC, and GelMA in the differentiation of ICOs toward hepatocyte-like cells. Furthermore, some trends indicate that an interplay of both the chemical composition and the mechanical properties has an influence on the relative expression of certain hepatocyte markers. Both DexNB-GelSH and CSNB-GelSH showed promising results for the expansion and differentiation of intrahepatic cholangiocyte organoids. The stiffest CSNB-GelSH hydrogel even significantly outperformed Matrigel based on ALB, BSEP, and CYP3A4 gene expression, being three important hepatocyte markers.

1. INTRODUCTION

Hepatic organoids are considered to be very promising in the field of liver tissue engineering, although they are still facing some limitations (e.g., lack of maturation, experimental variation) regarding their applications.[1] Organoids are especially of interest in the field of regenerative hepatology, for translational application or to gain insights into pathophysiology.[2] Especially the fact that organoids can be derived from human adult stem cells paves the way toward personalized liver research.[3] A major challenge in this regard is to selectively and fully differentiate liver organoids into hepatocyte-like cells, while existing differentiation protocols[4−6] to date result in organoids that show an immature phenotype rather than a mature one.[1]

In the current study, we focus on the development of highly defined matrices to support the expansion and subsequent differentiation of intrahepatic cholangiocyte organoids (ICOs).[7] These organoids are derived from intrahepatic cholangiocytes that adapt a bipotential stem cell phenotype in culture and have the potential to differentiate into hepatocyte- and cholangiocyte-like cells[8,9]

Received: December 19, 2022
Revised: December 14, 2023
Accepted: December 14, 2023
Published: January 4, 2024

Currently, the major limitations concerning the culture matrix of organoids include the malignant and animal-based origin, the high batch-to-batch variation, and the poorly defined composition, such as the standard used tumor matrices derived from Engelbreth−Holm−Swarm (EHS) sarcoma (e.g., Matrigel).[10] The culture matrix is of utmost importance since it does not only provide a 3D environment supporting organoid expansion but it can also influence cell fate via biomechanical cues (matrix stiffness and chemical composition).[11,12] Therefore, we focus herein on developing biomimetic culturing matrices that support organoid proliferation and improve the differentiation of ICOs toward hepatocyte-like cells and investigate the role of the biological as well as mechanical cues of the culture matrix in these processes.

Defined synthetic and nature-derived hydrogels for liver organoids were already described. In 2020, Krüger[13] et al. published on a cellulose nanofibril (CNF) hydrogel, which exhibited an improved differentiation potential compared to Matrigel. In the same year, a report was published on the polyisocyanopeptides, enriched with laminin−entactin complex (PIC-LEC).[14] Organoids cultured in this PIC-LEC hydrogel were highly proliferative, and the material exhibited a differentiation potential comparable to Matrigel. Substituting LEC with human recombinant laminin-111 rendered an animal-free material. Furthermore, the matrix stiffness is also a known important parameter as described by Sorrentino[15] et al. reporting on PEG hydrogels. However, contradictory results are reported[13−15] on the influence of matrix stiffness and ICOs' proliferation and differentiation potential. To date, there is no real consensus on this.

Another interesting material often used in liver tissue engineering is gelatin. Gelatin is derived from collagen being the major constituent of the ECM, but gelatin is less immunogenic,[16] highly processable,[17] and cost-effective,[18] while being cell-interactive.[19] Furthermore, its mechanical properties can be tuned by introducing (photo)cross-linkable moieties. Gelatin methacryloyl[20] (GelMA) is the most reported photo-cross-linkable gelatin derivative[21] and has already been described in the literature for bioprinting of ICO constructs serving drug toxicity applications with hepatic differentiation potential similar to Matrigel.[22]

In the present work, the advantages of gelatin are combined with those of a polysaccharide (mimicking the chemical nature of glycosaminoglycans present in the liver) by developing and exploiting homogeneous hybrid hydrogel networks constituting thiolated gelatin (GelSH) and norbornene-modified polysaccharides applying a thiol-norbornene step-growth cross-linking strategy.[23] As polysaccharides, dextran (Dex) was selected, since previous work revealed that a DexNB-GelSH hydrogel exhibited physicochemical properties (i.e., swelling, macro- and micromechanical properties) being in excellent agreement with those of natural liver tissue.[24] The latter thus enables us to investigate whether a hydrogel showing excellent physicochemical mimicry of the native liver is favorable to support ICO expansion and differentiation. On the other hand, chondroitin sulfate (CS) was selected since this is the second most abundant glycosaminoglycan present in the liver ECM. The latter enables us to investigate the influence of the presence of a liver-related GAG[25] in the hydrogel on the organoid response. The newly developed materials are investigated for their potential to serve as an alternative for Matrigel within the perspective of targeting future clinical applications.[26]

2. MATERIALS AND METHODS

2.1. Materials. Human intrahepatic cholangiocyte organoids (ICOs) were initiated and cultured from small liver tissue biopsies obtained during liver transplantation at the Erasmus MC Medical Center Rotterdam (n = 3). The use of tissues and cells for research purposes was approved by the Medical Ethical Council of the Erasmus MC (MEC-2014-060), and informed consent was provided by the liver transplant recipients. The approval and consent are in accordance with the ethical standard of the Helsinki Declaration of 1975.

Gelatin type B, isolated from bovine skin through an alkaline process, was supplied by Rousselot (Ghent, Belgium). Methacrylic anhydride, dextran (M_r ∼ 40 000 g/mol; dextran 40) from *Leuconostoc* spp., chondroitin-4-sulfate sodium salt from the bovine trachea, *N*-acetyl-homocysteine thiolactone, 5-norbornene-2-carboxylic acid, *N*,*N*′-dicyclohexylcarbodiimide (DCC), dimethylformamide (DMF), 4-(dimethylamino)-pyridine (DMAP), di*tert*-butyl dicarbonate (Boc_2O), ethylenediaminetetraacetic acid (EDTA) and Dowex 50 W proton exchange resin were purchased from Sigma-Aldrich. Spectrapor dialysis membranes with molecular weight cutoff (MWCO) 6−8 and 12−14 kDa were purchased from Polylab (Antwerp, Belgium).

Advanced DMEM/F12 (Gibco, Dublin, Ireland) supplemented with 1 v/v% penicillin−streptomycin (Gibco, Dublin, Ireland), 1 v/v % GlutaMax (Gibco, Dublin, Ireland), and 10 mM HEPES (Gibco, Dublin, Ireland) was used as the basic medium (AD+++) to make organoid initiation medium (OIM), expansion medium (EM), and differentiation medium (DM) and to wash organoids during passaging.

Other major materials used for organoid isolation and maintenance include type II collagenase (Gibco) and Dispase (Gibco), Matrigel (Corning, New York, NY, USA), nonattaching 24-well plates (M9312, Greiner, Merck). Certified fetal bovine serum (FBS) was obtained from Gibco (16000-044, origin: USA). OIM consisted of 70 v/v% EM and 30 v/v% Wnt-condition medium (homemade).

EM was made based on AD+++, supplemented with 2 v/v% B27 supplement without vitamin A (Invitrogen, Carlsbad, CA, USA), 1 v/v% N2 supplement (Invitrogen, Carlsbad, CA, USA), 10 mM nicotinamide (Sigma-Aldrich, St Louis, MO, USA), 1.25 mM *N*-acetylcysteine (Sigma-Aldrich, St Louis, MO, USA), 10 v/v% R-spondin-1 conditioned medium (the Rspo1-Fc-expressing cell line was a kind gift from Calvin J. Kuo), 10 μM forskolin (FSK, Sigma-Aldrich, St Louis, MO, USA), 5 μM A83-01 (transforming growth factor β inhibitor; Tocris Bioscience, Bristol, UK), 50 ng/mL EGF (Invitrogen, Carlsbad, CA, USA), 25 ng/mL HGF (Peprotech, Rocky Hill, NJ, USA), 0.1 μg/mL FGF10 (Peprotech, Rocky Hill, NJ, USA) and 10 nM recombinant human (Leu15)-gastrin I (Sigma-Aldrich, St Louis, MO, USA).

DM was purchased from Stem Cell Technologies, part of the HepatiCult Organoid Kit (Human).

Noviogel (polyisocyanopeptides, PIC) was purchased from Sopachem (1k-PIC-P, catalog numbers: NCN01). A stock solution of 5 mg/mL was made by adding 3 mL of AD+++ to each bottle of PIC. Laminin-entactin complex (LEC (10.5 mg/mL), Corning) was added to PIC to form functional PIC-LEC hydrogels.

Materials used for RNA isolation and qRT-PCR were the Trizol Reagent (Ambion, by Lifetechnologies, 15596018), iScript cDNA synthesis kit (Bio-Rad, 1708891), and iQ SYBR Green Supermix (Bio-Rad, 1708886). Primers were obtained from Eurogentec.

2.2. Development of Hydrogel Building Blocks. *2.2.1. Development of Methacrylamide-Modified Gelatin (GelMA).* GelMA was developed according to a protocol described earlier by Van Den Bulcke et al.[27] Briefly, 100 g of gelatin type B was dissolved in 1 L of 0.1 M phosphate buffer at pH 7.8 at 40 °C. A total of 2.5 equiv methacrylic anhydride were added relative to the amount of amines present in gelatin (i.e., 35.5 mmol/100 g gelatin). After 1 h of

https://doi.org/10.1021/acs.biomac.2c01496
Biomacromolecules 2024, 25, 590−604

continuous stirring, the reaction mixture was diluted with 1 L of double-distilled water. Purification was performed by dialysis using a MWCO membrane of 12−14 kDa for 24 h at 40 °C against distilled water. The final product was isolated by freeze-drying.

2.2.2. Development of Norbornene-Modified Dextran (DexNB). Dextran was modified with norbornene functionalities via conventional DCC/DMAP coupling chemistry between the hydroxyl groups of dextran and the carboxylic acid groups of NB (of 5- norbornene-2-carboxylic acid) according to a protocol described earlier.[24] Briefly, a total of 5 g of dextran (0.031 mol anhydroglucose units (AGU)) was dissolved in a mixture of 100 mL of dry DMF containing 10% w/v LiCl at 80 °C. After dextran was dissolved and the mixture was cooled to room temperature, 16.7 mmol of 5-norbornene-2-carboxylic acid, corresponding to 0.5 equiv with respect to the amount of AGU, was added. Subsequently, 12.3 mmol (0.4 equiv) of DMAP was added. After the mixture was cooled to 0 °C using an ice bath, 15.4 mmol (0.5 equiv) of *N*,*N*′-dicyclohexylcarbodiimide (DCC) was added. After 48 h reaction, impurities were precipitated in 500 mL of double-distilled water and filtered out. The filtrate was dialyzed using a MWCO membrane of 6−8 kDa over a period of 1 week against distilled water. The product was isolated by freeze-drying.

2.2.3. Development of Norbornene-Modified Chondroitin Sulfate (CSNB). Prior to the modification of CS with NB, CS was converted into its tetrabutylammonium salt (CS-TBA) to make it soluble in dimethyl sulfoxide (DMSO) based on a protocol by Abbadessa et al.[28] To develop CS-TBA, 10 g of CS was dissolved at a concentration of 2 w/v% in double distilled water, and 50 g of Dowex 50 W proton exchange resin was added to the solution, allowing exchange for 20 h. The resin was filtered off, and the filtrate was adjusted to a pH of 7 with TBA-OH. The resulting solution was frozen in liquid nitrogen, lyophilized, and stored at −20 °C until further use. To develop CSNB-TBA, CS-TBA was dissolved in anhydrous DMSO (10 w/v%). In order to develop CSNB with different degrees of substitution, a varying amount of Boc_2O and NB carboxylic acid was added. All reagents were dissolved in anhydrous DMSO prior to addition. 0.5, 1, 2, and 4 equiv 5-norbornene-2-carboxylic acid with respect to the amount of CS-TBA repeating units, and 0.5 equiv 4-(dimethylamino)pyridine were added while keeping the mixture under an argon atmosphere. The solution was heated to 45 °C after which 0.5, 1, 2, and 4 equiv of di*tert*-butyl dicarbonate (Boc_2O) were added by a syringe into the flask. After 20 h, cold water was added to quench the reaction. The mixture was purified by dialysis for 3 days against 150 mM NaCl to convert CS-TBA in its sodium salt and 4 more days against double distilled water, followed by freeze-drying.

2.2.4. Development of Thiolated Gelatin (GelSH). GelSH was developed according to a protocol described earlier by Van Vlierberghe et al.[29] Briefly, 10 g of gelatin type B was dissolved at 40 °C in 100 mL of 0.02 M carbonate buffer (pH 10). A total of 15 mM EDTA was added to the reaction mixture. Subsequently, 5 equiv of *N*-acetyl-homocysteine thiolactone were added to the reaction mixture followed by stirring for 3 h. After 3 h, 100 mL of double-distilled water was added and dialysis against distilled water was performed during 24 h at 40 °C under an inert argon atmosphere using a MWCO membrane of 12−14 kDa. After dialysis, the purified mixture was frozen by using liquid nitrogen and freeze-dried.

2.3. Hydrogel Building Block Characterization. *2.3.1. Proton Nuclear Magnetic Resonance (^{1}H NMR) Spectroscopy.* The degree of substitution (DS) of GelMA was determined using a 500 MHz Bruker Avance II Ascend ^{1}H NMR spectrometer at 40 °C. DexNB and CSNB were characterized using a 400 MHz Bruker Avance II Ultrashield ^{1}H NMR spectrometer at room temperature.

2.3.2. Ortho-Phthalic Dialdehyde (OPA) Assay. The OPA assay was used to quantify the number of amines present in a sample, enabling the calculation of the DS of the different gelatin derivatives. After dissolving 20 mg of OPA in 10 mL of ethanol, it was diluted to a final volume of 50 mL with double-distilled water. A second stock solution was prepared by adding 25 μL of 2-mercaptoethanol to 50 mL of borate buffer (0.1 M, pH 10). The reference contained 1000 μL of double-distilled water, 1500 μL of 2-mercaptoethanol solution, and 500 μL of the OPA solution. A calibration curve was obtained by comparing the reference samples to a sample containing 50 μL of *n*-butylamine standard solutions (0.002, 0.006, and 0.01 M), 950 μL of double-distilled water, 1500 μL of 2-mercaptoethanol solution, and 500 μL of the OPA solution. The absorbance of the samples at 335 nm was measured using a spectrophotometer, and a calibration curve was plotted. Solutions were made of gelatin type B, GelMA, and GelSH at a concentration of 25 mg/mL. Samples were measured with the spectrophotometer containing 50 μL of the gelatin solutions, 950 μL of double-distilled water, 1500 μL of 2-mercaptoethanol solution, and 500 μL of OPA solution at 335 nm. All measurements were performed in triplicate at 37 °C.

2.4. Covalent Hydrogel Cross-Linking. All hydrogels used throughout this work (i.e., GelMA, DexNB-GelSH, and CSNB-GelSH) were UV-A cross-linked in the presence of a photoinitiator (PI). The hydrogels were prepared starting from an aqueous solution with a total polymer concentration of 10 w/v% containing 2 mol % (with respect to the number of reactive moieties) of lithium phenyl-2,4,6-trimethylbenzoylphosphinate (Li-TPOL) as PI, followed by irradiation with UV-A light (10 mW/cm^2, 365 nm) during 30 min from both sides. All hydrogel solutions were prepared with equimolar reactive moieties, meaning that, except for GelMA, the number of thiols and norbornene functionalities are the same (i.e., #eq NB = #eq SH).

2.5. 2D Hydrogel Disc Fabrication. 2D hydrogel discs were prepared of the different hydrogels and were used to determine the gel fraction and the swelling ratio as well as to perform rheological frequency experiments and atomic force microscopy (AFM) measurements.

2D hydrogel films were prepared by injecting the polymer solutions (i.e., GelMA, DexNB-GelSH, and CSNB-GelSH) between two glass plates, which were separated by a 1 mm thick silicone spacer. The solutions were first exposed to 5 °C for 15 min to induce physical gelation, and afterward, UV-A (10 mW/cm^2, 365 nm) irradiation was applied for 30 min from both sides to induce chemical cross-linking. Subsequently, the films were incubated in a PBS buffer for 24 h. Subsequently, discs with a diameter of 11 mm were punched out to perform gel fraction and swelling tests.

2.6. Physicochemical Characterization. *2.6.1. Determination of Gel Fraction.* Hydrogel discs (Ø 11 mm) were freeze-dried after cross-linking and weighed. The obtained mass is the mass before leaching out of the non-cross-linked compounds (w_1). Swelling these samples for 24 h at 37 °C in double-distilled water and weighing them after another freeze-drying step resulted in the mass of the samples after leaching out of the non-cross-linked compounds (w_2). The gel fraction can be calculated by the following formula (n = 6):

$$\text{Gel fraction} = \frac{w_2}{w_1} \times 100$$

2.6.2. Determination of the Mass Swelling Ratio. The samples were weighed after freeze-drying (w_d) and after swelling for 24 h at 37 °C in PBS (w_s). The swelling ratio can be calculated using the following formula (n = 6):

$$\text{Swelling ratio} = \frac{(w_s - w_d)}{w_d}$$

2.6.3. Atomic Force Microscopy (AFM) Measurements. Atomic force microscopy (AFM) measurements were performed using a Nanowizard 4 instrument (JPK-bioAFM, Bruker) in order to analyze nanoscale mechanical properties. For all measurements, the DNP-10 (Bruker) chip was used combined with triangular cantilever A (hard samples: nominal spring constant 0.35 N/m) or cantilever C (soft samples: nominal spring constant 0.24 N/m). The AFM measurements were performed in quantitative imaging mode (QI mode). This mode allows the simultaneous gathering of information on morphological and mechanical properties. All data processing was performed using the JPK SPM DP software (image processing, roughness calculation, Young's modulus calculation). To calculate the

https://doi.org/10.1021/acs.biomac.2c01496
Biomacromolecules 2024, 25, 590−604

Table 1. List of Primers Used

target	forward primer	reverse primer	annealing temp [°C]	product size [bp]
GAPDH	CAAGATCATCAGCAATGCCT	CAGGGATGATGTTCTGGAGAG	60	194
RPL19	ATGAGTATGCTCAGGCTTCAG	GATCAGCCCATCTTTGATGAG	64	150
ALB	GTTCGTTACACCAAGAAAGTACC	GACCACGGATAGATAGTCTTCTG	64	144
BSEP	TTGAGACAATAGACAGGAAACC	TCTGGAAGGATAATGGAAGGT	60	116
CYP3A4	CACAGGCTGTTGACCATCAT	TTTTGTCCTATAAGGGCTTT	60	92
HNF4A	CATGTACTCCTGCAGATTTAGCC	CTTCCTTCTTCATGCCAGCC	60	110
MDR1	AATGATGCTGCTCAAGTTAAAGGG	TCAGTAGCGATCTTCCCAGAACC	60	239
MRP2	GCCAACTTGTGGCTGTGATAGG	ATCCAGGACTGCTGTGGGACAT	60	139
SLC10A1	GATATCACTGGTGGTTCTC	ATCATCCTCCCTTGATGAC	60	100
VTN	TGACCAAGAGTCATGCAAGGG	ACTCAGCCGTATAGTCTGTGC	60	116
LGR5	GCAGTGTTCACCTTCCC	GGTCCACACTCCAATTCTG	64	82
Ki67	GCTACTCCAAAGAAGCCTGTG	AAGTTGTTGAGCACTCTGTAGG	60	143
ECAD	AGGCCAAGCAGCAGTACATT	ATTCACATCCAGCACATCCA	60	110
KRT19	CTTCCGAACCAAGTTTGAGAC	AGCGTACTGATTTCCTCCTC	64	183

elasticity (Young's modulus [kPa]) of the samples, the Hertz/Sneddon model for parabolical indenters was used.

2.6.4. Rheological Characterization. For in situ photorheology (Physica MCR-301), 300 μL of each solution was placed between the plates of the device using a gap setting of 0.3 mm. An oscillation frequency of 1 Hz and a strain of 0.1% were applied. The samples were irradiated at 37 °C using UV-A light (10 min, 3500 mW/cm^2, 365 nm), followed by 2 min of postcuring monitoring. All measurements were performed in triplicate. Rheology on films was performed by punching out equilibrium swollen discs (Ø 14 mm) and placing them between the spindle (Ø 15 mm) and the bottom plate at 37 °C. A normal force of 1 N was applied on the discs. Subsequently, the storage modulus G' was monitored using an amplitude of 0.1% over a frequency range of 0.01−10 Hz. All measurements were performed in triplicate.

2.6.5. Degradation Assays. Hydrogel discs were prepared as described in 2.5. 2D Hydrogel Disc Fabrication and incubated in PBS buffer supplemented with 0.005 w/v% NaN_3 in a 48 multiwell plate at 37 °C. Every week, the gel fraction of the discs was determined. The measurements were performed in triplicate.

2.6.6. Swelling Experiments. Hydrogel discs were prepared as described in 2.5. 2D Hydrogel Disc Fabrication and freeze-dried. During 24 h, the discs were weighed at defined time points, and the swelling ratio was determined as described in '2.6.2. Determination of mass swelling ratio'.

2.7. Organoid Culture Protocol. *2.7.1. Organoid Isolation Protocol.* Human intrahepatic cholangiocyte organoid (ICO) lines were established and cultured as previously described.[6,7] Briefly, to establish organoid lines, liver tissues were cut into small pieces, followed by enzymatic digestion with 0.125 mg/mL type II collagenase and 0.125 mg/mL dispase in AD+++ containing 1 v/v % FBS. The supernatant was collected every hour. The procedure of tissue digestion and supernatant collection was repeated three times. Collected cells were washed in AD+++ containing 1 v/v% FBS and centrifuged at 450 × g for 5 min. The cells were resuspended in Matrigel at a concentration of ∼500 cells per μL, then seeded as droplets in nonattaching 24-well plates. OIM was added after approximately 15 min incubation at 37 °C, 5% CO_2.

2.7.2. Cell Culture Protocols. AD+++ medium was prepared by supplementing advanced DMEM/F12 with 1 v/v% penicillin-streptomycin, 1 v/v% GlutaMax and 10 mM HEPES.

Organoid initiation medium (OIM) was prepared using 70 v/v% EM and 30 v/v% Wnt-condition medium (homemade).

Expansion medium (EM) was made based on AD+++, supplemented with 2 v/v% B27 supplement without vitamin A, 1 v/v% N-2 supplement, 10 mM nicotinamide, 1.25 mM *N*-acetylcysteine, 10 v/v% R-spondin-1 conditioned medium, 10 μM forskolin, 5 μM A83−01, 50 ng/mL EGF, 25 ng/mL HGF, 0.1 μg/mL FGF10 and 10 nM recombinant human (Leu15)-gastrin I.

For the standard organoid culture, organoids were expanded and differentiated in Matrigel droplets. For organoid expansion, organoid cells (fragments) were plated within Matrigel droplets, and EM medium was added after gelation. The medium was changed every 2−3 days. Organoids were passaged by mechanical disruption once a week at an average split rate of 1:3−6 depending on density. In detail, when ICOs were almost confluent in Matrigel droplets, they were collected in 15 mL Eppendorf tubes containing cold AD+++. Then, the organoids were centrifuged at 4 °C at 450 × g for 5 min. After removing the supernatant, around 200 μL cold AD+++ was added to the tube by a pipet, and the organoids were disrupted mechanically by pipetting up and down until they were small clusters. After that, the tube was filled with cold AD+++ and centrifuged again to get a pellet of organoid cells. Once the supernatant was removed, the organoid cells were resuspended with Matrigel and plated in a 24-well plate (50 μL/well). EM was added (500 μL/well) after approximately 15 min incubation at 37 °C. All cultures were kept in a humified atmosphere containing 95% air and 5% CO_2 at 37 °C.

To differentiate ICOs into hepatocyte-like cells, the EM was changed to DM after 6 days of expansion. DM was changed every 2−3 days for 8 days.

2.7.3. Cell Encapsulation in Different Hydrogels. Matrigel, PIC, and LEC were thawed on ice for 1−2 h before use, and the gelatin-based hydrogels were prepared for use as described above. A stock solution of 5 mg/mL 1k-PIC-P was made by adding 3 mL of AD+++ to each bottle of PIC. LEC (10.5 mg/mL) was added to PIC to form the functional PIC-LEC hydrogels.

Organoid cells/fragments were collected via the same protocol as that used when passaging. Once organoid cells/fragments (3 donors and 6 tubes with cells/donor) were ready to be plated, 6 different hydrogels were added to the different tubes containing cell pellets (100 μL of hydrogel/donor/duplicate), respectively. The cells were mixed well with the hydrogels quickly and plated efficiently as droplets in 24-well plates. Final concentrations of each hydrogel used were: 100% Matrigel, PIC-LEC (1 mg/mL PIC-1K, 3 mg/mL LEC), GelMA (10 w/v%), DexNB-GelSH (10 w/v%), CSNB(12)-GelSH (10 w/v%), and CSNB(34)-GelSH (10 w/v%). Cells encapsulated in Matrigel and PIC-LEC hydrogels were incubated at 37 °C to solidify. Gelatin-based hydrogels were first physically cross-linked for 15 min at 4 °C and subsequently chemically cross-linked by irradiation with UV-A light (10 mW/cm^2, 365 nm) for 15 min in the presence of PI. Once the hydrogels became solid, EM was added (500 μL/well). Then, EM was refreshed every 2−3 days for 6 days. On day 6 (EM-D6), the medium was changed to DM (DM-D0), and DM was refreshed every 2 days until day 8 (DM-D8).

2.7.4. RNA Isolation and qRT-PCR Experiments. Trizol was used to isolate RNA from organoids following the manufacturer's instructions. First, 0.5 mL of Trizol was added to each well of organoids. After pipetting up and down a couple of times, the cell suspensions were transferred into 1.5 mL RNase-free Eppendorf

https://doi.org/10.1021/acs.biomac.2c01496
Biomacromolecules 2024, 25, 590−604

tubes. The rest of the procedures were applied as per the manufacturer's instructions. RNA quality and quantity were measured with a DS-11 spectrophotometer (DeNovix). Complementary DNA (cDNA) was synthesized with the iScript cDNA synthesis kit (Bio-Rad) following the manufacturer's instructions. Quantitative real-time PCR (qRT-PCR) was used to determine the relative expression of target genes using validated primers (Table 1) using the SYBR Green method (iQ SYBR Green Supermix, Bio-Rad). Normalization was carried out using the reference genes glyceraldehyde 3-phosphate dehydrogenase (*GAPDH*) and ribosomal protein L19 (*RPL19*).

2.7.5. Calcein AM Staining. After 8 days of differentiation, ICOs were incubated with Calcein AM (0.5 μM) and propidium iodide (50 μg/mL) at 37 °C and 5% CO_2 for 60 min. Organoids were imaged using an EVOS microscope (Thermofisher).

2.7.6. Microscopy and Immunofluorescence Analysis. Organoids harvested from the hydrogels on day 8 of differentiation were fixed in 4% (w/v) phosphate-buffered formaldehyde (PFA) for 45 min and embedded in 2.5 w/v% agar (BD). The organoids were dehydrated and embedded in paraffin. The embedded organoids were sectioned into 4 μm thin sections. For IF staining, the slides were incubated at 55 °C for 20 min and dewaxed by xylene, followed by rehydration in gradient alcohol concentrations from 100 to 70 v/v%. Then, samples were incubated in antigen retrieval solution at 98 °C for 30 min, followed by 30 min at RT. The sections were treated with 0.1 v/v% Triton X-100 (Sigma) in PBS for 10 min and blocked with 10 v/v% goat serum for 30 min. Next, primary antibodies were added to the slides and incubated overnight at 4 °C. The next day, the slides were washed three times with PBS containing 0.1 v/v% Tween-20 and incubated with secondary antibodies. Nuclei were counterstained with DAPI (0.5 μg/mL, Sigma-Aldrich). For each antibody, the antigen retrieval solution, dilutions, and corresponding secondary antibodies are summarized in Table 2.

Table 2. List of Antibodies Used

primary antibodies diluted in 10 v/v% normal goat serum (Sigma-Aldrich)					
antigen	source and cat. number	raised in	dilution	antigen retrieval	incubation
MDR1	Novus Bio NBP1-90291	rabbit	1:200	Tris–EDTA buffer for 30 min at 98 °C	O/N at 4 °C
albumin	Sigma A6684	mouse	1:1000		
CYP3A4	Abcam ab124921	rabbit	1:100		
keratin 18	Santa Cruz sc-51582	mouse	1:100		
MRP2	Abcam ab187644	rabbit	1:1000	citric acid buffer for 30 min at 98 °C	
E-cadherin	BD Bioscience 610181	mouse	1:100		
secondary antibodies diluted in 10% normal goat serum (Sigma-Aldrich)					
antigen	source and cat. number	raised in	dilution	incubation	
Antimouse Alexa 488	Invitrogen a11029	goat	1:200	1 h at RT	
Antirabbit Alexa 488	Invitrogen a11008				
Antimouse Alexa 568	Invitrogen a11004				
Antirabbit Alexa 568	Invitrogen a11036				

2.7.7. Rhodamine123 Transport Assay. For the rhodamine 123 transport assays, ICOs were differentiated for 8 days, as previously described. Organoids were treated with DM containing verapamil (10 μM reconstituted in DMSO, Sigma-Aldrich) or DMSO for 30 min. Organoids were then removed from the hydrogels and resuspended in DM containing rhodamine 123 (100 μM, Sigma-Aldrich) and incubated at 37 °C for 10 min. Fluorescence was imaged by using an EVOS FL cell imaging system (Life Technologies).

2.7.8. Albumin Production and L-Glutamate Dehydrogenase (GLDH) Expression. To quantify the intracellular levels of albumin (ALB) and GLDH, organoids were differentiated in the different hydrogels for 8 days, as previously described. DM was refreshed 24 h before the organoids were lysed in Milli-Q water. ALB and GLDH were measured in the cell lysates using a Beckman DxC-600 chemistry analyzer (Beckman Coulter). Values were normalized to the live cell numbers.

2.7.9. Ammonium Elimination Assay. Organoids were differentiated, as previously described. For ammonium elimination assays, organoids were incubated with DM supplemented with NH_4Cl (2 mM) for 24 h. After 24 h of incubation, media samples were harvested and stored at −20 °C. Tryple-Express (Gibco) was added to each well, and organoids were trypsinized for cell counting using the TC20 automated cell counter (Bio-Rad). Ammonium concentrations were measured with a urea/ammonia assay kit (Megazyme). As a control, DM containing NH_4Cl (2 mM) was incubated for 24 h without cells. Ammonia elimination rates were normalized to the live cell numbers.

2.7.10. Statistical Analysis. qRT-PCR results were analyzed using Tukey's multiple comparisons test by two-way ANOVA multiple comparisons. The *p*-values (significance set to 0.05) are indicated in the respective figures.

2.7.11. Data Availability. The data sets generated and analyzed during the current study are available from the corresponding author upon request.

3. RESULTS AND DISCUSSION

3.1. Hydrogel Development and Characterization. To determine the degree of substitution of GelMA and GelSH, an OPA assay was performed, which revealed a conversion of the amines of gelatin into methacrylamides and thiols of 93 and 65%, respectively. The data are in agreement with previous reports on gelatins modified through the same protocol.[27,29]

The modification degrees of Dex and chondroitin sulfate (CS) with norbornene moieties were quantified using ^{1}H NMR spectroscopy which revealed a DS of 16% for DexNB, which is in agreement with the literature.[24]

The modification of CS with NB involves a three-step reaction, for which the reaction scheme with the associated ^{1}H NMR spectra of the different intermediates is shown in Figure 1. First, the successful modification of chondroitin sulfate with TBAOH was confirmed by the characteristic peaks at 3.14, 1.61, 1.31, and 0.87 ppm corresponding to the hydrogen atoms of tetrabutylammonium (TBA).[28] Comparing these signals with the reference peak corresponding with the methyl hydrogens of the acetamide group on the *N*-acetylgalactosamine unit of CS evidenced the successful incorporation of 2.6 TBA moieties per disaccharide unit in CS-TBA, which is indicative of a slight excess of TBA present in the reaction mixture. The latter was taken into account for calculating the conversion toward CSNB-TBA.

The second step encompasses the reaction between the carboxylic acid group of 5-norbornene-2-carboxylic acid and the hydroxyl groups of CS-TBA using Boc_2O/DMAP coupling. In this step, different amounts of NB and Boc_2O were added to investigate the influence on the resulting degree of substitution. The resulting master curve showed a logarithmic correlation (Figure 2A) characterized by a correlation coefficient of 0.994. A simar trend was also reported before for the reaction between CS-TBA and glycidyl methacrylate (GMA) upon applying an increasing amount of GMA.[28]

The degree of substitution when adding 0.5, 1, 2, and 4 equiv was, respectively, 12, 34, 68, and 93%, with respect to the

https://doi.org/10.1021/acs.biomac.2c01496
Biomacromolecules 2024, 25, 590−604

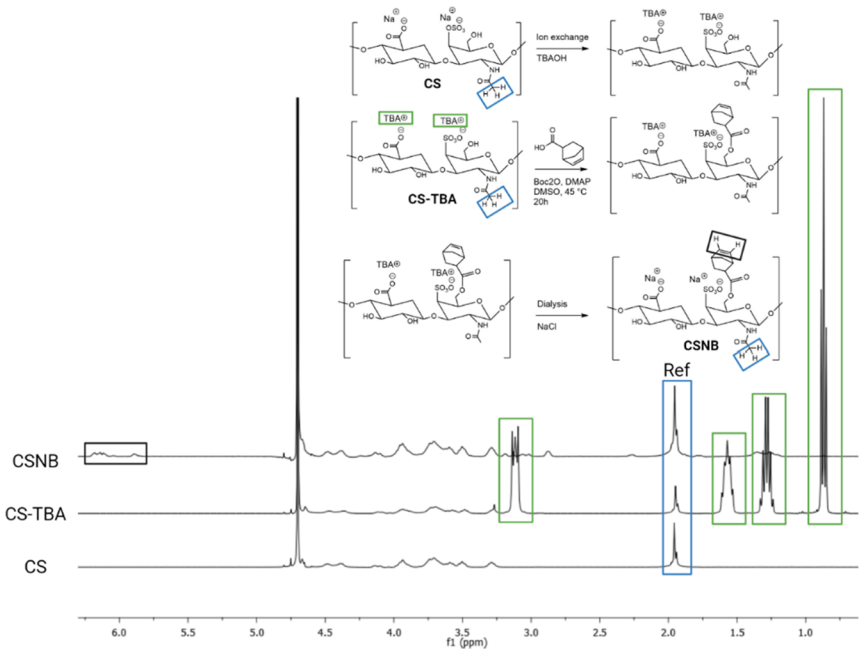

Figure 1. Reaction scheme showing the functionalization of chondroitin sulfate sodium salt with 5-norbornene-2-carboxylic acid using a Boc_2O/DMAP coupling together with the associated ^1H NMR spectra of the starting product and the different intermediates (i.e., chondroitin sulfate sodium salt, CS-TBA, and CS-NB) part of the norbornene-functionalization reaction of chondroitin sulfate.

disaccharide repeating units. The building blocks are from now onward referred to as CSNB(12), CSNB(34), CSNB(68), and CSNB(93). It should be noted that the DS of DexNB is defined as the percentage of modified monosaccharide units since dextran consists of anhydroglucose (i.e., monosaccharide) repeating units.

Subsequently, an in situ photorheology experiment was performed comparing GelMA, DexNB-GelSH, and CSNB-GelSH to gain insight into the photo-cross-linking efficiency and kinetics of CSNB-GelSH as compared to GelMA and DexNB-GelSH, being previously described in the literature[24] (Figure 2B).

CSNB-GelSH hydrogels exhibited slightly inferior cross-linking kinetics compared to the DexNB-GelSH hydrogel. This can be deduced from the initial steeper slope for the DexNB-GelSH hydrogel after UV onset compared with the CSNB-GelSH hydrogels. However, this cannot be quantified for DexNB-GelSH, since during the second time-point (between 72 and 84 s) there is already a significant decrease in cross-linking kinetics due to almost full cross-linking. For the different CSNB-GelSH hydrogels, there is also a difference in cross-linking kinetics. The slope of the curve obtained by the first 2 time points is for the CSNB(12)-GelSH, CSNB(34)-GelSH, CSNB(68)-GelSH, and CSNB(93)-GelSH respectively 328, 576, 552, and 280 (see Supporting Information S1). The highest kinetics are probably due to the combination of a high amount of norbornene moieties, but still enough mobility to enable efficient cross-linking. Furthermore, DexNB-GelSH also reached a plateau value faster being indicative of completed cross-linking.[30] The slower cross-linking of CSNB-GelSH in comparison with DexNB-GelSH might be caused by the negatively charged nature of chondroitin sulfate in combination with negatively charged gelatin above its iso-electric point (IEP) of 4.8−5.0,[31] which leads to a slower approaching of the polymer chains due to repulsive forces.[32,33] The latter phenomenon was described by Majcher et al. They executed research on the cross-linking kinetics of starch in uncharged, cationic, and anionic forms. Both the charged derivatives significantly increased the photoinduced gelation time.[34] However, all thiol-NB hydrogels exhibited faster cross-linking kinetics compared to GelMA. The latter was described before by Van Damme et al.[35] comparing the kinetics of GelMA with GelNB-GelSH hydrogels.

The storage modulus obtained after reaching a plateau provides information about the elasticity of the resulting hydrogels (see Supporting Information S2). The CSNB-GelSH hydrogels exhibited an up-to-threshold DS with a positive correlation between the DS and the elasticity of the material, albeit not linear. Indeed, more cross-linkable moieties result in a denser cross-linked network and lead to materials with higher elasticity. However, CSNB(93)-GelSH showed a decrease in elasticity. We hypothesize that upon exceeding a certain amount of NB moieties present, the thiol-NB reaction efficiency was reduced. The latter could potentially be related to excessive polymer hydrophobicity or sterical hindrance resulting from the NB groups, hence preventing efficient reaction with GelSH. Moreover, after a certain amount of cross-linkable moieties has reacted, mobility limitations could also occur thereby preventing the remaining moieties from reacting. To the best of our knowledge, no studies have been reported on NB-functionalized polysaccharides with a DS exceeding 60%.[36,37] The nonlinear behavior observed for CSNB-GelSH hydrogels with increasing norbornene modification, was also described earlier in publications describing research on the modification of gelatin[38] and hyaluronic acid[37] with NB moieties. The storage moduli of GelMA and CSNB(12)-GelSH were not significantly different ($p > 0.05$) while DexNB-GelSH showed the lowest storage modulus, in line with a previous report.[24] When a frequency sweep was performed on discs in a swollen state (see Figure 2C), CSNB-GelSH hydrogels exhibited a similar trend regarding mechanical behavior among each other. CSNB(68)-GelSH

https://doi.org/10.1021/acs.biomac.2c01496
Biomacromolecules 2024, 25, 590−604

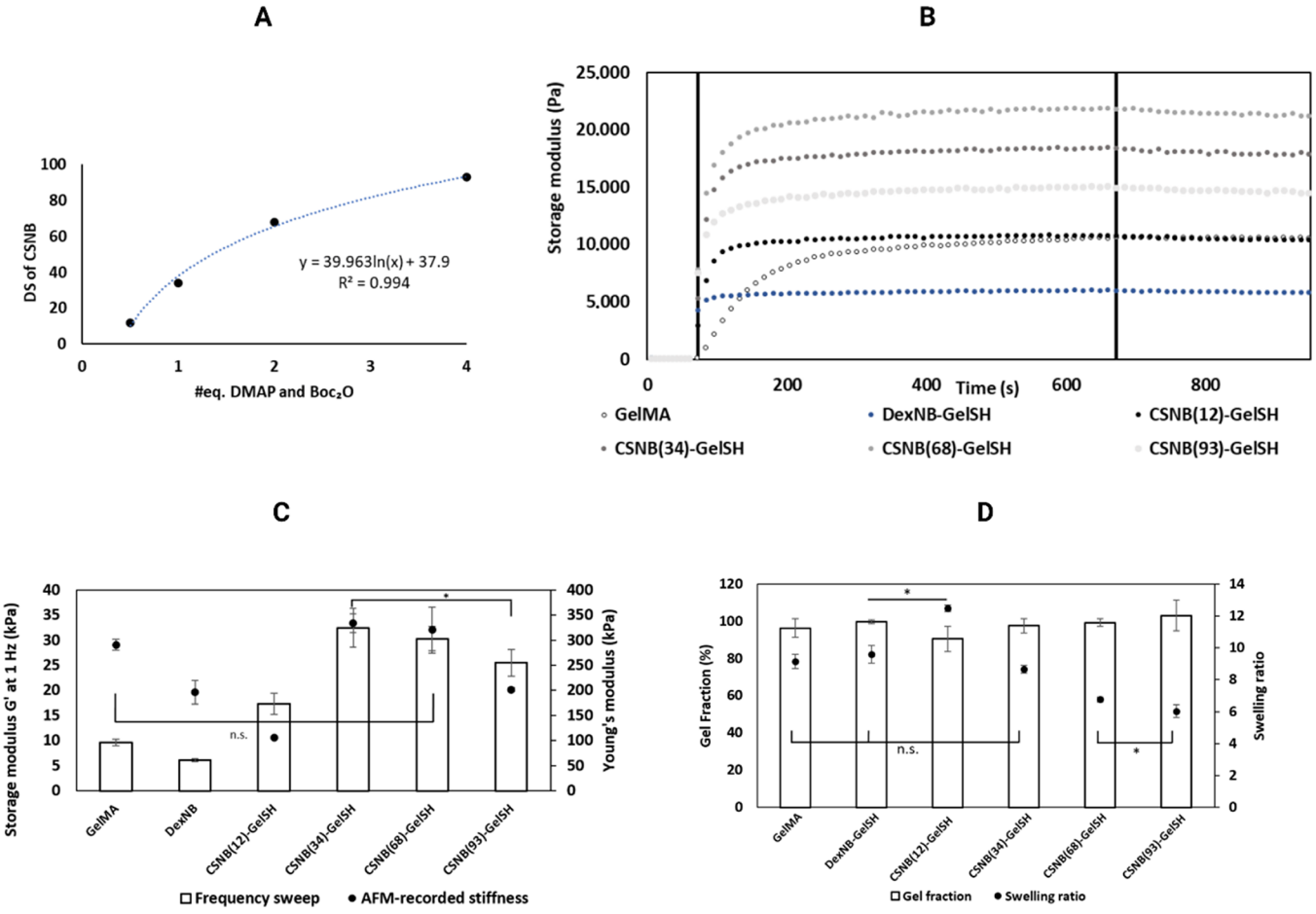

Figure 2. Overview of the physicochemical characterization of the developed CSNB-GelSH hydrogel. (A) Master curve representing the degree of substitution as a function of the amount of equivalents of DMAP and Boc_2O added during the modification of CS. (B) In situ photorheology of GelMA, DexNB-GelSH and the different CSNB-GelSH derivatives. (C) Summary of mechanical properties—storage moduli obtained via frequency sweep on equilibrium swollen hydrogel discs and quantification of the average Young's modulus of the hydrogels developed as determined using AFM (*$p > 0.05$). Error bars above indicate significant difference of the frequency sweep data, while the lower error bars indicate significant difference of the AFM-recorded stiffness. (D) Comparison of the mass swelling ratios and gel fractions between the different hydrogels (*$p > 0.05$). Error bars above indicate significant difference of the gel fraction, the lower error bars indicate significant difference of the swelling ratio data.

on the other hand exhibited inferior mechanical properties compared to CSNB(34)-GelSH, albeit not significant.

Another important parameter characterizing hydrogel materials serving tissue engineering includes stiffness. Hepatocytes are highly influenced by the mechanical properties of materials they are seeded on or encapsulated in.[39,40] The AFM-recorded stiffness is an adequate measure for the mechanical properties since it represents the stiffness on the microscale, implying that this represents the stiffness a cell is actually exhibited to.

It is known that the AFM-recorded stiffness of native liver tissue is ∼180 kPa,[40] which renders the DexNB-GelSH hydrogel an excellent candidate as a matrix for liver tissue engineering applications.[24] The results of the AFM measurements (see Figure 2C) evidenced a similar behavior among the CSNB-GelSH hydrogels, in agreement with the rheological data obtained via the frequency sweeps. Also, Young's moduli of GelMA and DexNB-GelSH were in agreement with the rheological data.

Next, gel fraction and swelling experiments (Figure 2D) were performed. The gel fraction provides information on the cross-linking efficiency, while the swelling ratio gives insight regarding the amount of water a hydrogel can absorb. Interestingly, the latter characteristic was also reported previously for liver tissue (i.e., 10),[41] hence enabling mimicry regarding this property.

The results showed that a higher DS resulted in higher gel fractions for the different CSNB-GelSH hydrogels. The highest gel fraction for CSNB(93)-GelSH might be counterintuitive based on the observed mechanical properties for CSNB(93)-GelSH. However, we hypothesize that in the case of the CSNB-GelSH materials with high DS, each CS chain contains enough NB moieties for at least one NB to react, hence becoming part of the gel fraction. GelMA exhibited the lowest gel fraction (albeit not significant), except for CSNB(12)-GelSH. It is known that step growth thiol-NB cross-linking chemistry is very efficient and generally results in higher gel fractions as compared to chain growth-induced methacrylamide-based cross-linking.[42] However, based on the gel fraction results obtained herein, the effect of efficient cross-linking appears to be inferior from a certain DS onward (i.e., lower than 12%) and the cross-linkable moieties will not reach each other anymore efficiently leading to lower gel fractions compared to GelMA.

https://doi.org/10.1021/acs.biomac.2c01496
Biomacromolecules 2024, 25, 590−604

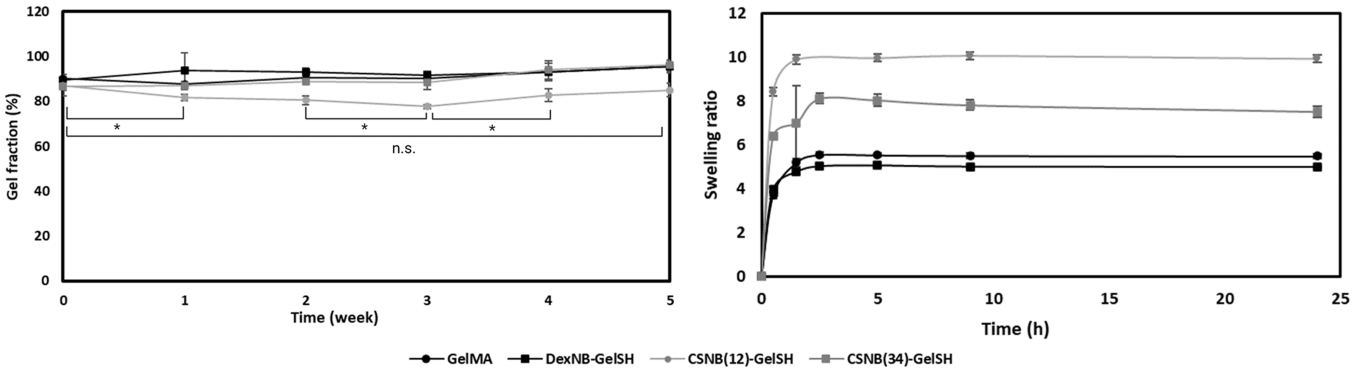

Figure 3. Results of the degradation study (left) and swelling experiments (right). *$p < 0.05$.

It should be noted that the DS of DexNB (i.e., 16%) is expressed with respect to the monosaccharide units present, which corresponds to 32% NB per disaccharide. Indeed, the gel fraction of DexNB-GelSH is most similar to that of CSNB(34)-GelSH. The latter observation also holds for the swelling ratio of both hydrogels. For the different CSNB-GelSH materials, the swelling ratio is the highest for the hydrogel containing CSNB with the lowest DS and the differences are more pronounced between the different CSNB-GelSH hydrogels in comparison to the gel fraction. This is due to a combination of the two factors. A higher DS results in a denser network leading to lower swelling,[43] while, on the other hand, the gel fraction also has an influence on the swelling behavior since lower gel fractions will result in more swelling.[44] CSNB(93)-GelSH showed the least swelling, resulting from the hydrophobic nature of the NB groups. GelMA exhibited a slightly lower swelling ratio compared with DexNB-GelSH, albeit not significant.

Taking into account the results of the physicochemical characterization, a selection of materials was made for the culture of ICOs to evaluate their potential regarding organoid expansion as well as their subsequent differentiation toward hepatocyte-like cells. DexNB-GelSH was selected since it mimics the physicochemical properties of the liver to a great extent (i.e., swelling ratio, macro- and microscale stiffness). Furthermore, CSNB(12)-GelSH and CSNB(34)-GelSH were selected since CS is a GAG that is present in the liver ECM, while both differ only in terms of their mechanical properties. The latter is studied herein since previous research regarding the importance of the mechanical properties gave different optimal stiffnesses for the proliferation and differentiation potential of encapsulated ICOs; however, the materials described were chemically different.[15,14] Hence, comparing CSNB(12)-GelSH and CSNB(34)-GelSH will elucidate the influence of the matrix mechanical properties on the cell behavior independent of the chemical composition. The comparison of DexNB-GelSH with CSNB(12)-GelSH on the other hand will provide information on the influence of the chemical composition since both hydrogels are similar regarding their mechanical properties. Matrigel is used as a benchmark throughout the study, and GelMA[22] and PIC-LEC[14] hydrogels are used as reference materials since they were already described before as potential materials for organoid culture.

On the selected materials (i.e., GelMA, DexNB-GelSH, CSNB(12)-GelSH, and CSNB(34)-GelSH), additional characterizations were performed. In addition to the gel fraction and the in situ photorheology quantitative data, the cross-linking degree was obtained using high-resolution magic angle spinning NMR spectroscopy (HR-MAS ^{1}H NMR). For the spectra, refer to Supporting Information S6. GelMA had a cross-linking degree of 52%. The chain-growth cross-linking mechanism associated with the photo-cross-linking of GelMA is known to be less efficient. The step-growth thiol-norbornene cross-linking is known to be much more efficient; however, it is not possible for the cross-linking degree to be exactly determined. For DexNB-GelSH the reference peak coincided partly with the solvent peak. Hence, only an estimation on the cross-linking degree can be made of 81%. The reference peaks of the CSNB(12)-GelSH and CSNB(34)-GelSH entirely coincided with the peaks of gelatin. However, in the spectrum of CSNB(12)-GelSH the norbornene peaks still appeared, while in the CSNB(34)-GelSH peaks they were completely gone. Interestingly, this was in line with the cross-linking efficiency observed during the in situ photorheology measurements and the gel fraction experiments of the different hydrogels.

A degradation study was performed in order to investigate the stability of the hydrogels in the physiological environment (i.e., in PBS at 37 °C) to ensure stable gels at least during the time required for the biological evaluation (see Figure 3, left). At the first time-point, there was no significant difference in gel fraction between the different materials. After 1 and 3 weeks, a significant reduction in gel fraction of CSNB(12)-GelSH was noticed, however, upon comparing the gel fraction on time-point 1 and time-point 6, no significant difference was seen. For the other materials, there was no significant reduction in gel fraction during 5 weeks. CSNB(12)-GelSH exhibited a significantly lower gel fraction compared to the other materials (except for time-point 1). There was no significant difference in gel fraction between GelMA, DexNB-GelSH and CSNB(34)-GelSH during the degradation assay of 5 weeks, which pointed toward the stability of the materials during the time needed for the biological evaluation. Finally, a swelling experiment was performed to investigate the swelling of the gels over time (Figure 3, right). This test revealed that equilibrium swelling occurred after 5 h. These results were in line with previous degradation and swelling experiments of gelatin-based hydrogels described in the literature.[45,46]

3.2. Biological Evaluation. Bright-field pictures were taken after 3 days of culturing the organoids in the different hydrogels in an expansion medium (EM) as shown in Figure 4. The organoids expanded in DexNB-GelSH and CSNB(12)-GelSH visually looked similar to those cultured in Matrigel and in the PIC-LEC hydrogel. Interestingly, DexNB-GelSH and CSNB(12)-GelSH are both hydrogels that have a similar

https://doi.org/10.1021/acs.biomac.2c01496
Biomacromolecules 2024, 25, 590−604

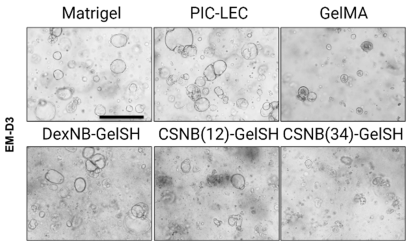

Figure 4. Bright-field images of the organoids encapsulated in the different hydrogels for 3 days in expansion medium (n = 3). Scale bar: 400 μm.

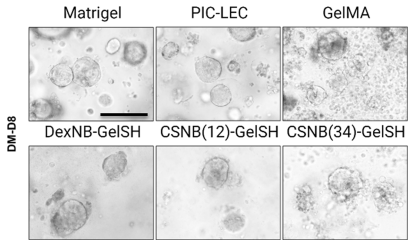

Figure 5. Bright-field images of the organoids encapsulated in the different hydrogels for 8 days in differentiation medium (n = 3). Scale bar: 200 μm.

AFM-recorded stiffness (i.e., respectively, 196 and 106 kPa) and are comparable to the stiffness of healthy native liver tissue (≈180 kPa).[47] The findings are in agreement with those of Sorrentino et al.[15] who reported on a better cell proliferation of organoids in a synthetic PEG-RGD matrix with a similar stiffness to healthy liver tissue. It should be noticed that the absolute values mentioned in this work are different compared to the values mentioned in some of the referenced studies. This is because the characterization technique is different (rheology vs AFM). In this work, AFM is used for characterization because the AFM-recorded stiffness of liver tissue is known and can be compared in that way. The stiffness measured with rheology however can also be compared, since in this work we additionally measured the storage modulus of the developed hydrogels using rheology (see Figure 2C). In general, all the hydrogels developed in this work are stiffer than the gels described by Sorrentino et al., with DexNB being the softest gel (i.e., 6.2 kPa measured via rheology). GelMA and CSNB(34)-GelSH hydrogels are much stiffer compared to healthy liver tissue (i.e., AFM recorded stiffness of 291 and 334 kPa, respectively, while rheology revealed a storage modulus of 9.6 and 32.5 kPa) and did not support the expansion of the organoids to the same extent. Organoids encapsulated in these materials remained very small and did not exhibit a noticeable proliferation. The latter is in line with our previous work where we observed that less stiff gels (i.e., 12 Pa, measured using rheology) were more suitable to support the proliferation of ICOs[14]. This is, however, in contrast with the findings of Sorrentino et al.,[15] who reported on less efficient proliferation in softer gels compared to native liver tissue. Organoids cultured in stiffer gels exhibited only limited proliferation, which was probably due to the limited migration ability of the cells throughout the gel. During expansion and proliferation cells self-organize into 3D hollow cystlike structures, the lower migration ability in stiffer gels limits this process.[48,49]

The subsequent differentiation toward hepatocyte-like cells was performed during 8 days in the differentiation medium (see Figure 5). As previously reported,[6,14] the organoids in all hydrogels were much darker and thicker in appearance. The darker and thicker appearance was not due to necrotic cell death as indicated by live−dead staining (see Supporting Information S3) but was indicative of organoid maturation, as described by Pleguezuelos-Manzano et al.[50]

Subsequent qPCR measurements (Figure 6) were performed to quantitatively assess the gene expression and associated degree of maturation. The newly developed hydrogels have a comparable performance compared to the Matrigel, PIC-LEC, and GelMA. Although mainly not being significantly different, some trends might be identified. There seems to be a trend toward a higher expression of the *LGR5* gene of organoids grown in DexNB-GelSH pointing toward a higher maintenance of the stem cell phenotype as compared to the other conditions, while the proliferative marker *Ki67* and the ductal marker *KRT19* were relatively less expressed in comparison with the other gels implying less proliferative character of the ICOs. Another trend is noticed in the stiffness. The higher the stiffness of the gel deviates from native liver tissue (i.e., more or less stiff), the higher the expression level of the *KRT19* gene. It appears that the chemical composition plays a minor role in this regard. Indeed, the CSNB(34)-GelSH has the highest stiffness, while PIC-LEC has a very low stiffness (compared using rheology), leading for both to a slight increase in expression of the *KRT19* gene, although not significant. It should be noted that Matrigel has an even higher expression of this marker, while its stiffness measured using rheology is between that of DexNB-GelSH (6.2 kPa) and PIC-LEC (i.e., 71 Pa).[14] However, since this is a very complex mixture, some other interfering biological cues could also play a role in this regard. Furthermore, it is known that Matrigel tends to support a high proliferation of organoids, even when grown in a differentiation medium.[51]

When considering the gene expression of mature hepatocyte markers, both chondroitin sulfate hydrogels were considered very promising (i.e., CSNB(12)-GelSH and CSNB(34)-GelSH). Most of the important mature hepatocyte markers (i.e., *ALB, BSEP, CYP3A4, MDR1,* and *MRP2*) were upregulated to a higher extent when chondroitin sulfate was incorporated and *KRT19* was downregulated compared to Matrigel and PIC-LEC, but upregulated compared to GelMA and DexNB-GelSH, the latter showing a more liver-related stiffness (i.e., 196 kPa). The upregulation of the hepatocyte markers, however not significant, points toward the fact that chondroitin sulfate might serve as a biological cue in the differentiation toward hepatocyte-like cells as it is known that *N*-galactosamine interacts with the ASGPR receptor on the cell surface inducing specific hepatocyte functions. In DexNB-GelSH, dextran can also act as a biological cue; however, this interaction is known to be less pronounced.[52] Furthermore, in the majority of the cases, a trend is seen toward upregulated hepatocyte markers (i.e., *ALB, BSEP, CYP3A4, MDR1,* and *MRP2*) for CSNB(34)-GelSH compared to CSNB(12)-GelSH indicating better maturation in the stiffer gel, which is in contrast with what was stated before by Sorrentino et al.[15] claiming that the stiffness did not impact the maturation. Important to note is the fact that the only common gene Sorrentino et al. considered was albumin which was more upregulated in the gel with the highest stiffness, albeit not significant due to high donor variability. Furthermore, this was also not in line with the work of Krüger et al.,[13] who reported that differentiation in softer gels rendered superior maturation

https://doi.org/10.1021/acs.biomac.2c01496
Biomacromolecules 2024, 25, 590−604

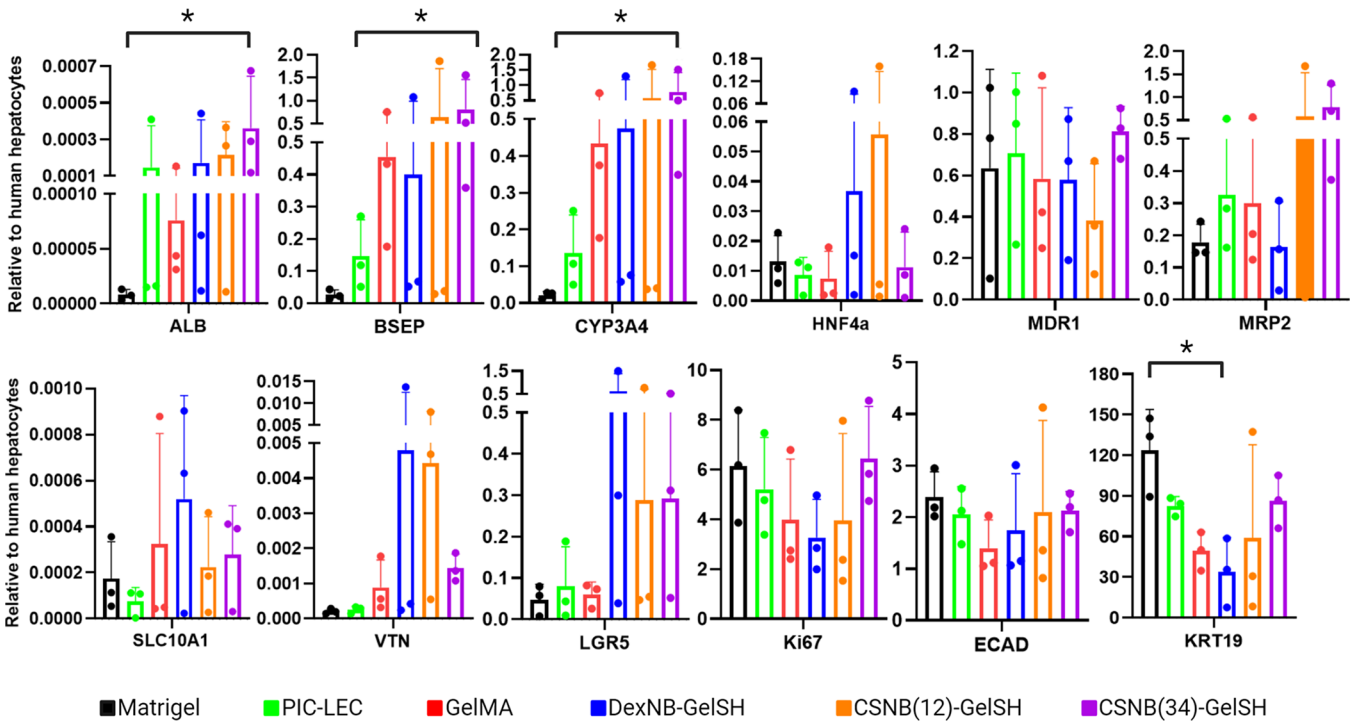

Figure 6. Gene expression of hepatocyte markers after 8 days of organoid culture in DM, encapsulated in the different hydrogels. Shown is the mean and standard deviation of the relative gene expression as compared to the expression in primary human hepatocytes as determined via qPCR. $n = 3$ ($^*p < 0.05$).

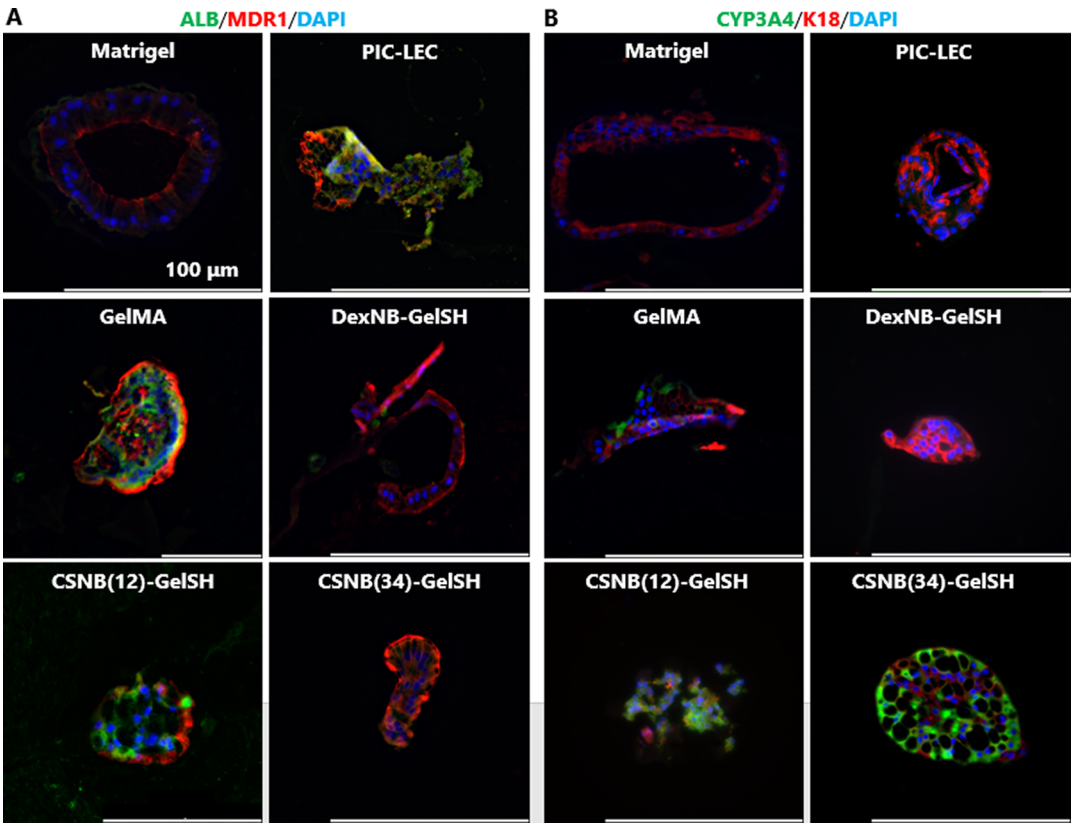

Figure 7. Immunofluorescent analysis of paraffin-embedded organoids confirmed that the organoids in all hydrogels expressed hepatic functional proteins. (A) Albumin (ALB, in green) and multidrug-resistance-associated protein 1 (MDR1, in red). (B) Cytochrome p450 3A4 (CYP3A4, green) and keratin 18 (K18, in red). 4′,6-Diamidino-2-phenylindole (DAPI for nuclei, in blue). Scale bars = 100 μm. $n = 3$.

https://doi.org/10.1021/acs.biomac.2c01496
Biomacromolecules 2024, 25, 590−604

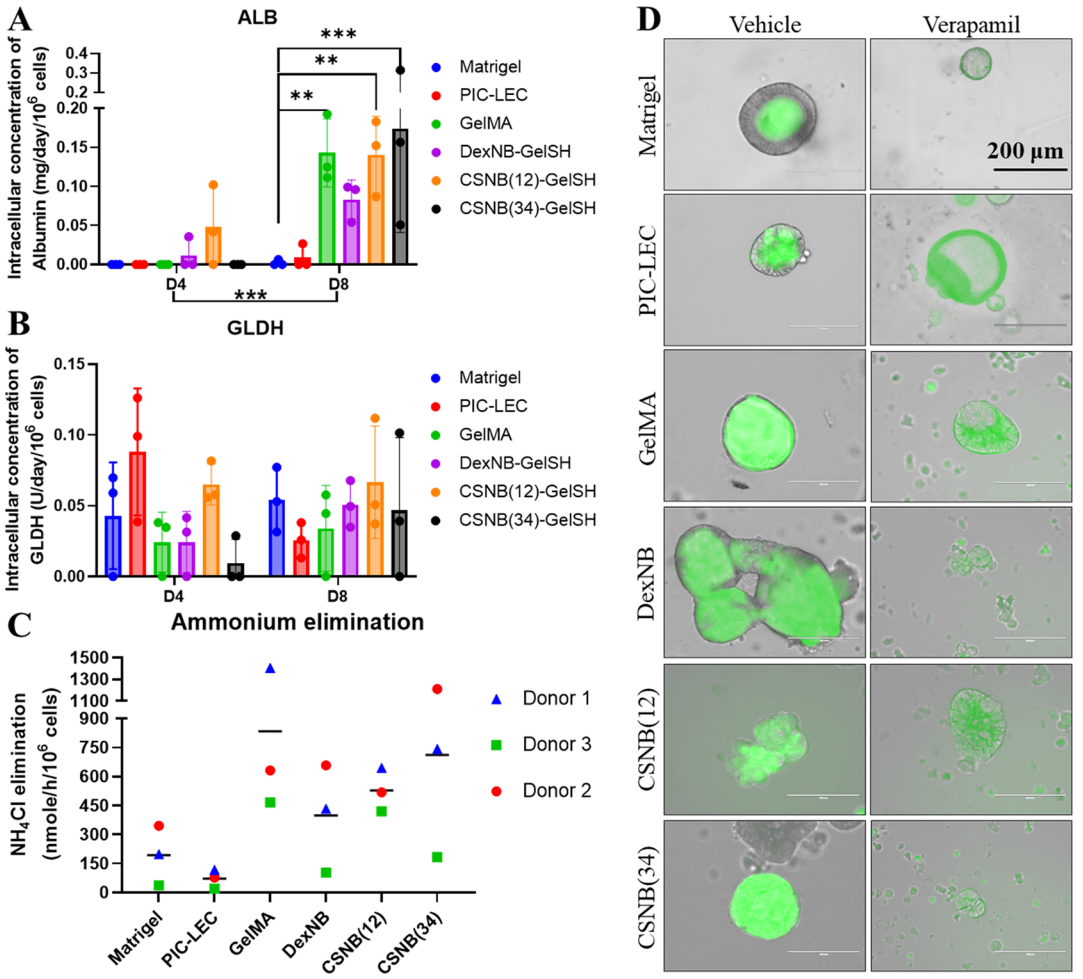

Figure 8. Organoids differentiated into functional hepatocyte-like cells in different hydrogels. (A) Albumin (ALB) concentrations and (B) GLDH levels in cell lysates were measured after 8 days of differentiation (fresh DM was added 24 h before sample collection). The protein concentrations were normalized to the cell numbers. Graphs indicate the mean ± SD. The asterisk indicates p-value ≤0.05. Hydrogels DexNB-GelSH, CSNB(12)-GelSH, and CSNB(34)-GelSH were respectively labeled as DexNB, CSNB(12), and CSNB(34) in C and D. (C) Ammonium elimination from the culture medium was determined as a read-out for hepatocyte functionality (fresh DM supplemented with NH_4Cl was added 24 h before sample collection). (D) Rhodamine 123 (green) transport was determined as a read-out for MDR1 activity. Verapamil was added as an inhibitor of the MDR1 function. Scale bars = 200 μm.

of ICOs. Interestingly, in this work, CSNB(34)-GelSH even outperformed Matrigel as evidenced by the significant upregulation of *ALB*, *BSEP*, and *CYP3A4* gene expression, being three important hepatocyte markers.

This trend of the higher upregulation of the hepatocyte markers in case of introducing CS and a higher stiffness, however, is not true for all studied genes. The hepatocyte markers *HNF4A* and *VTN*, were mainly affected by the stiffness, and not by the chemical composition. Here, a relatively higher expression was noticed when the AFM-recorded stiffness approached the stiffness (≈180 kPa) of native liver tissue (i.e., for DexNB-GelSH and CSNB(12)-GelSH). Finally, a trend is seen between the stiffness and the *KRT19* expression, while the chemical composition only seems to have a minor influence. More specifically, upon approaching liver stiffness, this marker was downregulated.

Some genes might be more stiffness-sensitive, while others might be more regulated by biological cues. This could also be a possible explanation for the contradictory results reported in the literature. Indeed, often different genes are considered to assess the maturation of organoids, and the composition of the described materials also varies. It is clear, however, that the expansion and differentiation of ICOs require different material properties. More in-depth research should be performed in the future to provide a conclusive answer in this regard.

In addition to the gene expression levels characterized by qPCR, we further verified the presence of hepatic proteins by immunofluorescence (IF) staining assays. IF staining for hepatic markers confirmed the maturation of ICOs toward hepatocyte-like cells. ICOs differentiated in PIC-LEC, GelMA, and CSNB(12)-GelSH expressed albumin (Figure 7A). MDR1 was clearly expressed in PIC-LEC, GelMA, DexNB-GelSH, CSNB(12)-GelSH, and CSNB(34)-GelSH conditions on the outside of the ICOs (Figure 7A). The MDR1 expression in Matrigel was not as clearly detected but seemed to be mainly expressed on the luminal side of the ICOs (Figure 7A). Interestingly, CYP3A4 was abundantly expressed in ICOs cultured in CSNB(12)-GelSH and CSNB(34)-GelSH, and expressed in some cells cultured in GelMA, while being absent under Matrigel and PIC-LEC conditions (Figure 7B). Keratin 18 and E-cadherin were expressed in all conditions and seem to show hexagonal cell morphology (Figure 7B and Supporting Information S4).

https://doi.org/10.1021/acs.biomac.2c01496
Biomacromolecules 2024, 25, 590−604

No necrotic core death could be observed in any of the ICOs after 8 days of differentiation using Calcein AM and propidium iodide staining (Supporting Information S3). E-Cadherin was also clearly present in the center of the ICOs, suggesting no necrotic core (Supporting Information S4).

Intracellular GLDH and albumin levels were assessed to determine the degree of maturation. Albumin concentration was not detectable or very low for all samples on day 4 of differentiation (Figure 8A). After 8 days of differentiation, albumin levels were upregulated in all samples compared to day 4, with significantly higher levels in GelMA, CSNB(12)-GelSH, and CSNB(34)-GelSH compared to Matrigel. On the other hand, the protein levels of GLDH remained stable and comparable between D4 and D8 (Figure 8B) in all conditions. However, the concentration of GLDH was variable, both between donors and the various hydrogels after both 4 and 8 days of differentiation.

To further investigate the functional maturation of ICOs, ammonium elimination capacity was assessed. Overall, ICOs cultured in GelMA, DexNB-GelSH, CSNB(12)-GelSH, and CSNB(34)-GelSH showed a trend of higher elimination capacity than ICOs cultured in Matrigel and PIC-LEC.

Since we detected MDR1 on the protein level, we further investigated the functionality of MDR1 with a rhodamine 123 transport assay. To determine functional transmembrane transport, we exposed organoids in all hydrogels to rhodamine 123 (Rh123), a fluorescent compound secreted from the apical membrane of hepatocytes by MDR1. ICOs in all hydrogels accumulated fluorescence in their lumen. To show that this accumulation was MDR1 specific, ICOs were pretreated with verapamil, a competitive inhibitor of MDR1. This resulted in fluorescence in the cytoplasm of the cells and no fluorescence in the lumen of the ICOs (Figure 8D). To be noted, for some ICOs, the location of MDR1 was different in the novel developed hydrogels compared to that in Matrigel (Figure 7A), suggesting that the polarity of some but not all ICOs differentiated in these hydrogels was reversed. Accordingly, some ICOs in the novel hydrogels showed no accumulation of Rh123 in the lumen (Supporting Information S5) while others showed comparable luminal Rh123 accumulation as the Matrigel control, mediated by functional MDR1 on the membrane facing the lumen of the ICOs (Figure 8D).

4. CONCLUSIONS AND FUTURE PERSPECTIVES

In the current research, two newly developed hydrogel materials were proposed as possible alternatives to Matrigel, namely, DexNB-GelSH and CSNB-GelSH with different degrees of CSNB modification (resulting in different stiffnesses). The influence on the proliferation and differentiation of ICOs encapsulated in these materials was investigated.

The results showed that a hydrogel exhibiting lower stiffness (and comparable to that of native liver tissue ≈180 kPa) supports the expansion of organoids to a greater extent as compared to stiffer hydrogels (GelMA and CSNB(34)-GelSH hydrogels with stiffness of respectively 291 and 334 kPa). Hydrogels with lower mechanical properties (i.e., Matrigel and PIC-LEC) even gave rise to the formation of larger organoids.

The results of the qPCR analysis revealed a higher trend of expression of important mature hepatocyte markers (i.e., *ALB, BSEP, CYP3A4, MDR1,* and *MRP2*) in the novel developed materials compared to Matrigel and PIC-LEC, particularly in the gels where chondroitin sulfate was incorporated. Importantly, also on protein level, CYP3A4 was abundantly detected in CSNB(12)-GelSH and CSNB(34)-GelSH, while being absent in Matrigel and PIC-LEC. To the best of our knowledge, this is the first time that CYP3A4 was detected in ICOs on a protein level. This improved maturation toward hepatocyte-like cells in our novel hydrogels was further substantiated by the increase in intracellular albumin concentrations. The increase in intracellular albumin concentration for all hydrogels except Matrigel and PIC-LEC between days 4 and 8 of differentiation (Figure 8A) suggests that this increased maturation occurred mainly between days 4 and 8 of differentiation. Intracellular GLDH concentrations did not differ between the different hydrogels (Figure 8B), however, the ammonium elimination rate showed a trend of higher elimination in the gelatin-based hydrogels compared to Matrigel and PIC-LEC (Figure 8C). Moreover, a subset of organoids differentiated in the novel developed hydrogels reversed their polarity, as indicated by MDR1 expression on the outside of the ICOs, indicating that these functional organoids better represent the in vivo situation.

In conclusion, although the expansion of organoids in the gelatin-based hydrogels needs further improvement, the differentiation of organoids in these hydrogels is very promising. For instance, introducing chondroitin sulfate gave a trend toward a higher expression of some major hepatocyte markers and an increased hepatocyte functionality compared to Matrigel, while an increased stiffness even supports the maturation to a greater extent resulting in a significantly higher upregulation of *ALB, BSEP*, and *CYP3A4* in CSNB(34)-GelSH compared to Matrigel.

A combination of materials with both physical properties (i.e., DexNB-GelSH) and chemical properties (i.e., CSNB-GelSH) matching native liver tissue looks very promising to replace Matrigel for the expansion and maturation of ICOs as both processes seemed to be guided by an interplay between mechanical and biological cues of the matrix.

It is clear, however, that expansion and differentiation do require other material properties, which will be the subject of forthcoming research. Ideally, future research should focus either on materials that can easily be degraded in order to isolate organoids after expansion to transfer to another gel supporting the differentiation or on materials that can change properties over time. In the latter case, there is no need for disruption of the material to transfer organoids from an expansion-promoting gel to a differentiation-promoting gel.

The proposed hydrogels in this work are very promising. However, future research should include a thorough investigation of the functionality of liver cells and their application in drug-screening models. Also, the ability to process encapsulated organoids into relevant 3D constructs exploiting 3D-printing techniques will be the topic of forthcoming studies.

■ ASSOCIATED CONTENT

Supporting Information

The Supporting Information is available free of charge at https://pubs.acs.org/doi/10.1021/acs.biomac.2c01496.

In situ photo-cross-linking; storage moduli; live−dead staining; immunofluorescent staining; rhodamine 123 transport assay; and HR-MAS ^{1}H-NMR spectra (PDF)

https://doi.org/10.1021/acs.biomac.2c01496
Biomacromolecules 2024, 25, 590−604

AUTHOR INFORMATION

Corresponding Authors

Kerstin Schneeberger − *Department Clinical Sciences, Faculty of Veterinary Medicine, Utrecht University, Utrecht 3584 CT, The Netherlands*; Email: k.schneeberger@uu.nl

Sandra Van Vlierberghe − *Polymer Chemistry & Biomaterials Group, Centre of Macromolecular Chemistry, Department of Organic and Macromolecular Chemistry, Ghent University, Ghent 9000, Belgium*; orcid.org/0000-0001-7688-1682; Email: sandra.vanvlierberghe@ugent.be

Authors

Nathan Carpentier − *Polymer Chemistry & Biomaterials Group, Centre of Macromolecular Chemistry, Department of Organic and Macromolecular Chemistry, Ghent University, Ghent 9000, Belgium*; orcid.org/0000-0002-7985-4310

Shicheng Ye − *Department Clinical Sciences, Faculty of Veterinary Medicine, Utrecht University, Utrecht 3584 CT, The Netherlands*

Maarten D. Delemarre − *Department Clinical Sciences, Faculty of Veterinary Medicine, Utrecht University, Utrecht 3584 CT, The Netherlands*

Louis Van der Meeren − *Nano-Biotechnology Laboratory, Department of Biotechnology, Faculty of Bioscience Engineering, Ghent University, Ghent 9000, Belgium*; orcid.org/0000-0002-6671-5055

André G. Skirtach − *Nano-Biotechnology Laboratory, Department of Biotechnology, Faculty of Bioscience Engineering, Ghent University, Ghent 9000, Belgium*; orcid.org/0000-0002-4468-7620

Luc J. W. van der Laan − *Department of Surgery, Erasmus MC-University Medical Center, Rotterdam 3000 CA, The Netherlands*

Bart Spee − *Department Clinical Sciences, Faculty of Veterinary Medicine, Utrecht University, Utrecht 3584 CT, The Netherlands*

Peter Dubruel − *Polymer Chemistry & Biomaterials Group, Centre of Macromolecular Chemistry, Department of Organic and Macromolecular Chemistry, Ghent University, Ghent 9000, Belgium*

Complete contact information is available at: https://pubs.acs.org/10.1021/acs.biomac.2c01496

Author Contributions

⊥N.C. and S.Y. contributed equally.

Notes

The authors declare no competing financial interest.

ACKNOWLEDGMENTS

N.C. would like to acknowledge the Research Foundation Flanders (FWO) for providing him with an FWO-SB fellowship (3S99321N). A.G.S. acknowledges the support of FWO (I002620N). S.Y. acknowledges the support of the China Scholarship Council (CSC201808310180). TOC was created with BioRender.com.

REFERENCES

(1) Harrison, S. P.; Baumgarten, S. F.; Verma, R.; Lunov, O.; Dejneka, A.; Sullivan, G. J. Liver Organoids: Recent Developments, Limitations and Potential. *Front. Med.* **2021**, *8*, No. 574047.

(2) Jalan-Sakrikar, N.; Brevini, T.; Huebert, R. C.; Sampaziotis, F. Organoids and regenerative hepatology. *Hepatology* **2023**, *77*, 305−322.

(3) Zhu, X.; Zhang, B.; He, Y.; Bao, J. Liver Organoids: Formation Strategies and Biomedical Applications. *Tissue Eng. Regen. Med.* **2021**, *18*, 573−585.

(4) Broutier, L.; Andersson-rolf, A.; Hindley, C. J.; Boj, S. F.; Clevers, H.; Koo, B.; Huch, M. Culture and establishment of self-renewing human and mouse adult liver and pancreas 3D organoids and their genetic manipulation. *Nat. Protoc.* **2016**, *11*, 1724−1743.

(5) Huch, M.; Boj, S. F.; Clevers, H. Lgr5+ liver stem cells, hepatic organoids and regenerative medicine. *Regen. Med.* **2013**, *8*, 385−387.

(6) Schneeberger, K.; Sánchez-Romero, N.; Ye, S.; van Steenbeek, F. G.; Oosterhoff, L. A.; Pla Palacin, I.; Chen, C.; van Wolferen, M. E.; van Tienderen, G.; Lieshout, R.; Colemonts-Vroninks, H.; Schene, I.; Hoekstra, R.; Verstegen, M. M. A.; van der Laan, L. J. W.; Penning, L. C.; Fuchs, S. A.; Clevers, H.; De Kock, J.; Baptista, P. M.; Spee, B. Large-Scale Production of LGR5-Positive Bipotential Human Liver Stem Cells. *Hepatology* **2020**, *72*, 257−270.

(7) Marsee, A.; Roos, F. J. M.; Verstegen, M. M. A.; H. P. B. O. Consortium; Gehart, H.; De, E.; Forbes, S. J.; Peng, W. C.; Huch, M.; Takebe, T.; Vallier, L.; Clevers, H.; van der Laan, L. J. W.; Spee, B. Building consensus on definition and nomenclature of hepatic, pancreatic, and biliary organoids. *Cell Stem Cell* **2021**, *28*, 816−832.

(8) Huch, M.; Gehart, H.; Van Boxtel, R.; Hamer, K.; Blokzijl, F.; Verstegen, M. M. A.; Ellis, E.; Van Wenum, M.; Fuchs, S. A.; De Ligt, J.; Van De Wetering, M.; Sasaki, N.; Boers, S. J.; Kemperman, H.; De Jonge, J.; Ijzermans, J. N. M.; Nieuwenhuis, E. E. S.; Hoekstra, R.; Strom, S.; Vries, R. R. G.; Van Der Laan, L. J. W.; Cuppen, E.; Clevers, H. Long-term culture of genome-stable bipotent stem cells from adult human liver. *Cell* **2015**, *160*, 299−312.

(9) Aloia, L.; Mckie, M. A.; Vernaz, G.; Cordero-espinoza, L.; Aleksieva, N.; Van Den Ameele, J.; Antonica, F.; Font-cunill, B.; Raven, A.; Cigliano, R. A.; Belenguer, G.; Mort, R. L.; Brand, A. H.; Zernicka-goetz, M.; Forbes, S. J.; Miska, E. A.; Huch, M. Epigenetic remodelling licences adult cholangiocytes for organoid formation and liver regeneration. *Nat. Cell Biol.* **2019**, *21*, 1321−1333.

(10) Kaur, S.; Kaur, I.; Rawal, P.; Tripathi, D. M.; Vasudevan, A. Non-matrigel scaffolds for organoid cultures. *Cancer Lett.* **2021**, *504*, 58−66.

(11) Saheli, M.; Sepantafar, M.; Pournasr, B.; Farzaneh, Z.; Vosough, M.; Piryaei, A.; Baharvand, H. Three-dimensional liver-derived extracellular matrix hydrogel promotes liver organoids function. *J. Cell. Biochem.* **2018**, *119*, 4320−4333.

(12) Ng, S. S.; Saeb-Parsy, K.; Blackford, S. J. I.; Segal, J. M.; Serra, M. P.; Horcas-Lopez, M.; No, D. Y.; Mastoridis, S.; Jassem, W.; Frank, C. W.; Cho, N. J.; Nakauchi, H.; Glenn, J. S.; Rashid, S. T. Human iPS derived progenitors bioengineered into liver organoids using an inverted colloidal crystal poly (ethylene glycol) scaffold. *Biomaterials* **2018**, *182*, 299−311.

(13) Krüger, M.; Oosterhoff, L. A.; Van Wolferen, M. E.; Schiele, S. A.; Walther, A.; Geijsen, N.; De Laporte, L.; Van Der Laan, L. J. W.; Kock, L. M.; Spee, B. Cellulose Nanofibril Hydrogel Promotes Hepatic Differentiation of Human Liver Organoids. *Adv. Healthcare Mater.* **2020**, *9*, No. 1901658.

(14) Ye, S.; Boeter, J. W. B.; Mihajlovic, M.; van Steenbeek, F. G.; van Wolferen, M. E.; Oosterhoff, L. A.; Marsee, A.; Caiazzo, M.; van der Laan, L. J. W.; Penning, L. C.; Vermonden, T.; Spee, B.; Schneeberger, K. A Chemically Defined Hydrogel for Human Liver Organoid Culture. *Adv. Funct. Mater.* **2020**, *30*, No. 2000893.

(15) Sorrentino, G.; Rezakhani, S.; Yildiz, E.; Nuciforo, S.; Heim, M. H.; Lutolf, M. P.; Schoonjans, K. Mechano-modulatory synthetic niches for liver organoid derivation. *Nat. Commun.* **2020**, *11*, 3416.

(16) Lynn, A. K.; Yannas, I. V.; Bonfield, W. Antigenicity and immunogenicity of collagen. *J. Biomed. Mater. Res., Part B: Appl. Biomater.* **2004**, *71*, 343−354.

(17) Yin, J.; Yan, M.; Wang, Y.; Fu, J.; Suo, H. 3D Bioprinting of Low-Concentration Cell-Laden Gelatin Methacrylate (GelMA) Bioinks with a Two-Step Cross-linking Strategy. *ACS Appl. Mater. Interfaces* **2018**, *10*, 6849−6857.

(18) Ye, S.; Boeter, J. W. B.; Penning, L. C.; Spee, B.; Schneeberger, K. Hydrogels for liver tissue engineering. *Bioengineering* **2019**, *6*, No. 59.
(19) De Moor, L.; Fernandez, S.; Vercruysse, C.; Tytgat, L.; Asadian, M.; De Geyter, N.; Van Vlierberghe, S.; Dubruel, P.; Declercq, H. Hybrid Bioprinting of Chondrogenically Induced Human Mesenchymal Stem Cell Spheroids. *Front. Bioeng. Biotechnol.* **2020**, *8*, No. 484.
(20) Van Den Bulcke, A. I.; Bogdanov, B.; De Rooze, N.; Schacht, E. H.; Cornelissen, M.; Berghmans, H. Structural and Rheological Properties of Methacrylamide Modified Gelatin Hydrogels. *Biomacromolecules* **2000**, *1*, 31−38.
(21) Van Hoorick, J.; Tytgat, L.; Dobos, A.; Ottevaere, H.; Van Erps, J.; Thienpont, H.; Ovsianikov, A.; Dubruel, P.; Van Vlierberghe, S. (Photo-) crosslinkable gelatin derivatives for biofabrication applications. *Acta. Biomater.* **2019**, *97*, 46−73.
(22) Bouwmeester, M. C.; Bernal, P. N.; Oosterhoff, L. A.; van Wolferen, M. E.; Lehmann, V.; Vermaas, M.; Buchholz, M. B.; Peiffer, Q. C.; Malda, J.; van der Laan, L. J. W.; Kramer, N. I.; Schneeberger, K.; Levato, R.; Spee, B. Bioprinting of Human Liver-Derived Epithelial Organoids for Toxicity Studies. *Macromol. Biosci.* **2021**, *21*, No. e2100327.
(23) Lin, C.-C.; Ki, C. S.; Shih, H. Thiol-norbornene photo-click hydrogels for tissue engineering applications. *J. Appl. Polym. Sci.* **2015**, *132*, No. 41563.
(24) Carpentier, N.; Van Der Meeren, L.; Skirtach, A. G.; Devisscher, L.; Van Vlierberghe, H.; Dubruel, P.; Van Vlierberghe, S. Gelatin-Based Hybrid Hydrogel Scaffolds: Toward Physicochemical Liver Mimicry. *Biomacromolecules* **2023**, *24* (10), 4333−4347.
(25) Gressner, A. M.; Krull, N.; Bachem, M. G. Regulation of Proteoglycan Expression in Fibrotic Liver and Cultured Fat-Storing Cells. *Pathol. Res. Pract.* **1994**, *190*, 864−882.
(26) Aisenbrey, E. A.; Murphy, W. L. Synthetic alternatives to Matrigel. *Nat. Rev. Mater.* **2020**, *5*, 539−551.
(27) Van Den Bulcke, A. I.; Bogdanov, B.; De Rooze, N.; Schacht, E. H.; Cornelissen, M.; Berghmans, H. Structural and rheological properties of methacrylamide modified gelatin hydrogels. *Biomacromolecules* **2000**, *1*, 31−38.
(28) Abbadessa, A.; Blokzijl, M. M.; Mouser, V. H. M.; Marica, P.; Malda, J.; Hennink, W. E.; Vermonden, T. A thermo-responsive and photo-polymerizable chondroitin sulfate-based hydrogel for 3D printing applications. *Carbohydr. Polym.* **2016**, *149*, 163−174.
(29) Van Vlierberghe, S.; Schacht, E.; Dubruel, P. Reversible gelatin-based hydrogels: Finetuning of material properties. *Eur. Polym. J.* **2011**, *47*, 1039−1047.
(30) Stubbe, B.; Mignon, A.; Van Damme, L.; Claes, K.; Hoeksema, H.; Monstrey, S.; Van Vlierberghe, S.; Dubruel, P. Photo-Crosslinked Gelatin-Based Hydrogel Films to Support Wound Healing. *Macromol. Biosci.* **2021**, *21*, No. 2100246.
(31) Johnston-Banks, F. A. *Food gels*; Harris, P., Ed.; Elsevier: Sutton Weaver, Runcorn, Cheshire, 1990; pp 233−289.
(32) Patil, S. V.; Dhanraj, J. Crosslinking Of Polysaccharides: Methods And Applications. *Pharm. Rev.* **2008**, *6*, 1−11.
(33) Blöhbaum, J.; Paulus, I.; Pöppler, A. C.; Tessmar, J.; Groll, J. Influence of charged groups on the cross-linking efficiency and release of guest molecules from thiol-ene cross-linked poly(2-oxazoline) hydrogels. *J. Mater. Chem. B* **2019**, *7*, 1782−1794.
(34) Majcher, M. J.; Himbert, S.; Vito, F.; Campea, M. A.; Dave, R.; Vetergaard Jensen, G.; Rheinstadter, M. C.; Smeets, N. M. B.; Hoare, T. Investigating the Kinetics and Structure of Network Formation in Ultraviolet-Photopolymerizable Starch Nanogel Network Hydrogels via Very Small-Angle Neutron Scattering and Small-Amplitude Oscillatory Shear Rheology. *Macromolecules* **2022**, *55*, 7303−7317.
(35) Van Damme, L.; Van Hoorick, J.; Blondeel, P.; Van Vlierberghe, S. Toward Adipose Tissue Engineering Using Thiol-Norbornene Photo- Crosslinkable Gelatin Hydrogels. *Biomacromolecules* **2021**, *22*, 2408−2418.
(36) McOscar, T. V. C.; Gramlich, W. M. Hydrogels from norbornene-functionalized carboxymethyl cellulose using a UV-initiated thiol-ene click reaction. *Cellulose* **2018**, *25*, 6531−6545.
(37) Xiao, X.; Huang, Z.; Jiang, X.; Yang, Y.; Yang, L.; Yang, S.; Niu, C.; Xu, Y.; Feng, L. Facile synthesize of norbornene-hyaluronic acid to form hydrogel via thiol-norbornene reaction for biomedical application. *Polymer (Guildf).* **2022**, *245*, No. 124696.
(38) Göckler, T.; Haase, S.; Kempter, X.; Pfister, R.; Maciel, B. R.; Grimm, A.; Molitor, T.; Willenbacher, N.; Schepers, U. Tuning Superfast Curing Thiol-Norbornene-Functionalized Gelatin Hydrogels for 3D Bioprinting. *Adv. Healthcare Mater.* **2021**, *10*, No. 2100206.
(39) You, J.; Park, S. A.; Shin, D. S.; Patel, D.; Raghunathan, V. K.; Kim, M.; Murphy, C. J.; Tae, G.; Revzin, A. Characterizing the effects of heparin gel stiffness on function of primary hepatocytes. *Tissue Eng. - Part A* **2013**, *19*, 2655−2663.
(40) Xia, T.; Zhao, R.; Feng, F.; Yang, L. The Effect of Matrix Stiffness on Human Hepatocyte Migration and Function—An In Vitro Research. *Polymers* **2020**, *12*, No. 1903.
(41) Mattei, G.; Di Patria, V.; Tirella, A.; Alaimo, A.; Elia, G.; Corti, A.; Paolicchi, A.; Ahluwalia, A. Mechanostructure and composition of highly reproducible decellularized liver matrices. *Acta Biomater.* **2014**, *10*, 875−882.
(42) Van Hoorick, J.; Gruber, P.; Markovic, M.; Rollot, M.; Graulus, G. J.; Vagenende, M.; Tromayer, M.; Van Erps, J.; Thienpont, H.; Martins, J. C.; Baudis, S.; Ovsianikov, A.; Dubruel, P.; Van Vlierberghe, S. Highly Reactive Thiol-Norbornene Photo-Click Hydrogels: Toward Improved Processability. *Macromol. Rapid Commun.* **2018**, *39*, No. 1800181.
(43) Sievers, J.; Sperlich, K.; Stahnke, T.; Kreiner, C.; Eickner, T.; Martin, H.; Guthoff, R. F.; Schünemann, M.; Bohn, S.; Stachs, O. Determination of hydrogel swelling factors by two established and a novel non-contact continuous method. *J. Appl. Polym. Sci.* **2021**, *138*, No. 50326.
(44) Daoud, M.; Bouchaud, E.; Jannink, G. Swelling of Polymer Gels. *Macromolecules* **1986**, *19*, 1955−1960.
(45) Sharifi, S.; Sharifi, H.; Akbari, A.; Chodosh, J. Systematic optimization of visible light - induced crosslinking conditions of gelatin methacryloyl (GelMA). *Sci. Rep.* **2021**, *11*, No. 23276.
(46) Heltmann-Meyer, S.; Steiner, D.; Müller, C.; Schneidereit, D.; Friedrich, O.; Salehi, S.; Engel, F. B.; Arkudas, A.; Horch, R. E. Gelatin methacryloyl is a slow degrading material allowing vascularization and long-term use in vivo. *Biomed. Mater.* **2021**, *16*, No. 065004.
(47) Zhao, G.; Cui, J.; Qin, Q.; Zhang, J.; Liu, L.; Deng, S.; Wu, C.; Yang, M.; Li, S.; Wang, C. Mechanical stiffness of liver tissues in relation to integrin β1 expression may influence the development of hepatic cirrhosis and hepatocellular carcinoma. *J. Surg. Oncol.* **2010**, *102*, 482−489.
(48) Mattei, G.; Magliaro, C.; Giusti, S.; Ramachandran, S. D.; Heinz, S.; Braspenning, J.; Ahluwalia, A. On the adhesion-cohesion balance and oxygen consumption characteristics of liver organoids. *PLoS One* **2017**, *12*, No. e0173206.
(49) Xia, T.; Zhao, R.; Liu, W.; Huang, Q.; Chen, P.; Waju, Y. N.; Al-ani, M. K.; Lv, Y.; Yang, L. Effect of substrate stiffness on hepatocyte migration and cellular Young's modulus. *J. Cell. Physiol.* **2018**, *233*, 6996−7006.
(50) Pleguezuelos-manzano, C.; Puschhof, J.; Van Den, S.; Geurts, V.; Beumer, J.; Clevers, H. Establishment and Culture of Human Intestinal Organoids Derived from Adult Stem Cells. *Curr. Protoc. Immunol.* **2020**, *130*, No. e106.
(51) Bernal, P. N.; Bouwmeester, M.; Madrid-Wolff, J.; Falandt, M.; Florczak, S.; Rodriguez, N. G.; Li, Y.; Größbacher, G.; Samsom, R. A.; van Wolferen, M.; van der Laan, L. J. W.; Delrot, P.; Loterie, D.; Malda, J.; Moser, C.; Spee, B.; Levato, R. Volumetric Bioprinting of Organoids and Optically Tuned Hydrogels to Build Liver-Like Metabolic Biofactories. *Adv. Mater.* **2022**, *34*, No. 2110054.
(52) Zhang, Y.; Zhou, T.; Luo, L.; Cui, Z.; Wang, N.; Shu, Y.; Wang, K. P. Pharmacokinetics, biodistribution and receptor mediated

https://doi.org/10.1021/acs.biomac.2c01496
Biomacromolecules 2024, 25, 590−604

endocytosis of a natural Angelica sinensis polysaccharide. *Artif. Cells, Nanomedicine Biotechnol.* **2018**, *46*, 254−263.

https://doi.org/10.1021/acs.biomac.2c01496
Biomacromolecules 2024, 25, 590−604